LBL-11037

Lawrence Berkeley Laboratory
UNIVERSITY OF CALIFORNIA

Engineering & Technical
Services Division

Presented at the IEEE Nuclear Science Symposium, Orlando, FL, November 5-7, 1980; and to be published in IEEE Transactions on Nuclear Science

SEMICONDUCTOR DETECTORS FOR MEDICAL TOMOGRAPHY WITH HIGH-ENERGY HEAVY IONS

Jorge Llacer, Eugen E. Haller, William L. Hansen, John T. Walton, and Eleanor K. Batho

November 1980

Prepared for the U.S. Department of Energy under Contract W-7405-ENG-48

SEMICONDUCTOR DETECTORS FOR MEDICAL TOMOGRAPHY
WITH HIGH-ENERGY HEAVY IONS

LBL-11037

Jorge Llacer, Eugen E. Haller, William L. Hansen,
John T. Walton and Eleanor K. Batho
Lawrence Berkeley Laboratory
University of California
Berkeley, California 94720

Summary

High-energy heavy ion beams are in use at the Lawrence Berkeley Laboratory for cancer therapy. In order to take full advantage of the very favorable depth-dose characteristics of those beams, it is necessary to determine the stopping characteristics of the ions in the complex media of a human with greater accuracy than obtainable with X-ray CAT scanning. Initial measurements with an array of Si dE/dx position sensitive detectors and a windowless thin planar Ge detector used in a side entry mode show the potential for fabricating an instrument for high accuracy on-line CAT scanning using the same ions to be used for therapy. It is estimated that one tomography can be obtained with a dose of 0.72 Rad-gm.

Introduction

High-energy heavy ion beams are being used in a variety of basic and applied biomedical studies at the Lawrence Berkeley Laboratory. These studies include cell, tissue and organ radiobiology, cancer detection (radiography) and therapy. In the particular case of cancer therapy, very sophisticated techniques based on the results of X-ray computerized axial tomographic (CAT) scanning of the regions to be treated are used to define treatment plans so as to deliver the maximum dose to the tumor regions, sparing the surrounding healthy tissue regions. The sharply peaked dose-depth characteristics of energetic heavy ions beams (Fig. 1 for 224 MeV/n ^{16}O) are very favorable for the treatment of small tumors in regions close to sensitive organs, in cases where surgery or chemotherapy are not effective or possible. The utilization of the sharp Bragg peak for therapy requires the use of very accurate data for the treatment plan. It is desirable to know the heavy ion stopping characteristics in the complex media in a patient with cumulative errors as small as perhaps 1 mm. The use of sophisticated X-ray tomographic techniques, with a very well calibrated instrument, may provide information of tissue density and composition with cumulative errors of no more than a few millimeters for regions of the body without internal motion. This accuracy is adequate for most therapy applications, but not for cases in which high precision beam delivery is required.

Research at LBL on radiography with heavy ions[1] has shown that the absence of beam hardening, the excellent separability of nuclear vs ionizing interactions, as opposed to the difficulty of separating photoelectric vs Compton effects in X-rays, and the shallow angle scattering of heavy ion beams result in an excellent potential for very high accuracy tomographic imaging with low radiation doses.Further, the ability to obtain fast on-line tomographic images with heavy ions for a patient positioned for therapy, using the same ion beam which is going to be used for therapy is deemed of great value. Verification of treatment planning parameters and corrections for organ position changes between the time of x-ray tomography and therapy would then be possible just prior to irradiation.

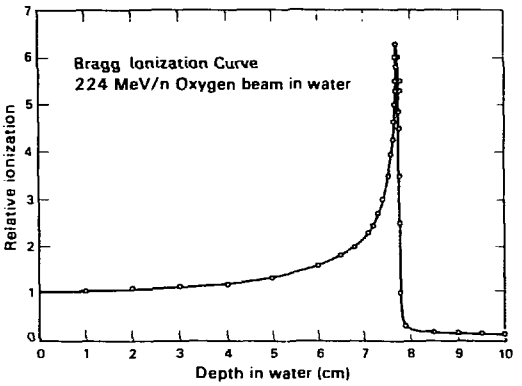

Fig. 1. Relative Ionization Curve for a 224 MeV per nucleon ^{16}Oxygen beam in water. The narrow Bragg peak corresponds to the point where the ion beam causes maximum cell destruction in a cancer therapy application.

The availability of thin silicon ion-implanted resistive sheet position sensitive, fully depleted detectors and of a very stable surface coating for germanium detectors without any apparent surface dead layers have allowed us to plan and test a configuration of detectors which will allow the design and construction of an instrument for fast on-line tomographic image acquisition and reconstruction. It is the purpose of this paper to report the results of the initial measurements with the chosen detector configuration, to discuss the relevant parameters which will make those detectors useful for a high accuracy-low dose tomographic reconstruction, and to show the results of a preliminary image reconstruction effort.

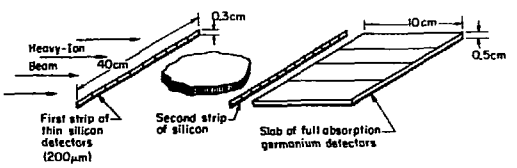

Fig. 2 Schematic design of a solid-state detector heavy-ion tomograph. The object to be imaged is to rotated after sufficient data have been acquired to generate one projection.

General Approach

Figure 2 shows schematically the approach taken for the design of a complete instrument for a single slice tomographic reconstruction. The first position sensitive detectors determine the time and position of arrival of each ion in the beam. After traversing the

subject to be imaged, the ions are detected in the second position sensitive detector in time coincidence with the first detector. If an individual ion has not suffered a deviation larger than a certain predetermined amount, it will be accepted for further processing. Germanium detectors, also in time coincidence, will measure the full residual energy of the ions. Knowledge of position and residual energy for all accepted ions provides the raw data for image reconstruction. Residual energy can be converted to a water equivalent thickness of the object to be imaged by using the initial beam energy and a table look up procedure. Water equivalent thickness is a very convenient parameter for image reconstruction with heavy ions since the obtained values are practically invariant with ion species and energy. The reconstructed image is finally a tomographic slice with values in a pixel which are the average stopping power of the contents of the pixel with respect to water for heavy ions. These results can be applied directly to radiation treatment planning.

Detector Characteristics

Three Si dE/dx detectors have been fabricated for the initial tests. Their thickness is 200 micrometers approximately, with a transverse length of 30 mm and a height of 5 mm. They operate fully depleted with an alpha-particle resolution of approximately 70 keV FWHM. The detectors have been made from p-type material, with a P diffused n-contact and a B implanted resistive p-contact with a resistance of 5 K (end-to-end). Depletion voltage is approximately 60 V. Position resolution, limited by electronic noise, is 0.3 mm FWHM with ^{12}C ions. Figure 3 shows a dE/dx spectrum for a beam of 425 MeV/n ^{20}Ne after passing through 6 cm of water. The Landau-shaped primary particle spectrum is observable, as well as peaks corresponding to a number of secondary particles generated by nuclear fragmentation in the water absorber.

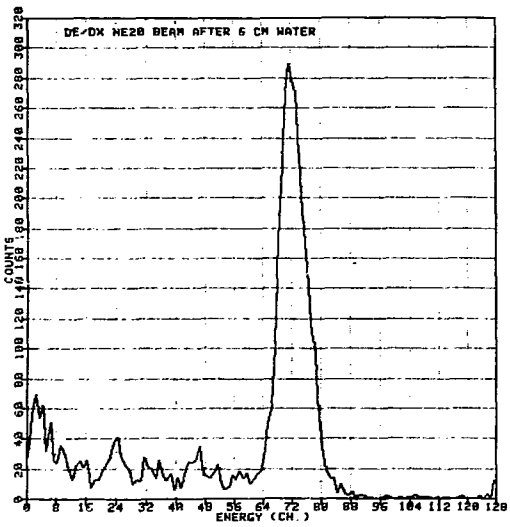

Fig. 3 dE/dx spectrum for a ^{20}Ne beam of 425 MeV/n after passing through 6 cm of water. The peak occurs at approximately 10 MeV of deposited energy on 200 μm of Si.

Two Ge full absorption detectors have been studied. Initially, a one-cm thick planar detector was placed in the beam with the ions entering through the thin ion implanted p-type contact. The energy of the ion beam was modulated with a water absorber so that the Bragg peak of the ions was located inside the detector. With 400 MeV/n ^{12}C ions, the main peak of the ion energy spectrum was of Gaussian shape with a FWHM of 5 MeV/n. With 3500 particles in the spectrum, the centroid of the peak could be determined with an expected error of 0.01 cm water, or approximately 0.04% of a 25 cm water phantom (human head equivalent).

Radiation damage experiments showed that the detector remained in excellent condition until a total fluence of 2 x 10^8 particles/cm^2 after which it deteriorated rapidly. Complete recovery was obtained after a routine anneal at 150°C for a few hours. The energy spectra of the damaged detector indicated heavy trapping for both holes and electrons at the precise region of the sharp Bragg peak (Fig. 1) inside the detector during the radiation.

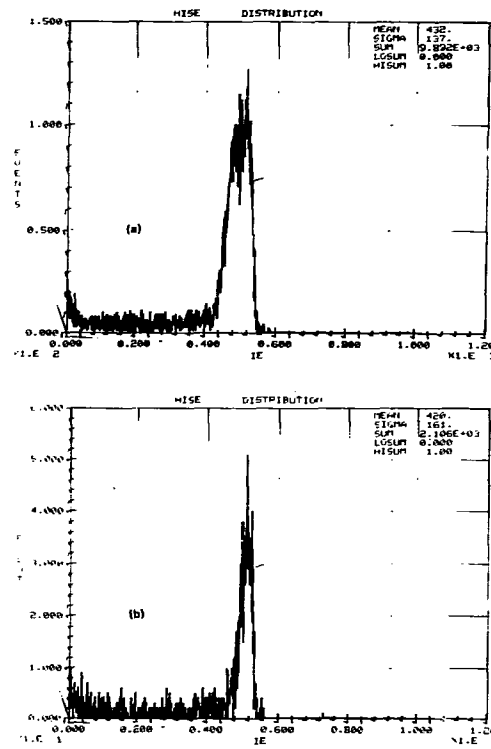

Fig. 4 Residual energy spectrum for a 150 MeV/n ^{12}C ion beam for a side-entrance detector without surface coating. a) Full 5 mm detector height is illuminated by the beam. b) Only 2 mm nearest the p-contact of detector height were illuminated by ion beam.

A second Ge detector with a more practical configuration has been investigated next. Because of the thickness of Ge needed for an instrument with sufficient dynamic range, it is necessary to consider flat detectors with side entrance. For that purpose, a detector of 3.5 cm length (in the beam direction) with a thickness of 0.5 cm and a width of 2.3 cm (transverse to the beam) was fabricated. As anticipated, the surface dead layers created a very large disturbance in the obtained residual energy spectra by virtue of their non-uniformity. Figure 4a shows a typical spectrum for side entrance when the total lateral surface was illuminated by a 150 MeV/n ^{12}C beam.

Figure 4b shows the corresponding spectrum when only the lower half of the detector surface was illuminated. The observed surface behavior rendered this Ge detector practically useless for the high accuracy residual energy determination needed in the project. A guard ring structure was also tried, with even worse results.

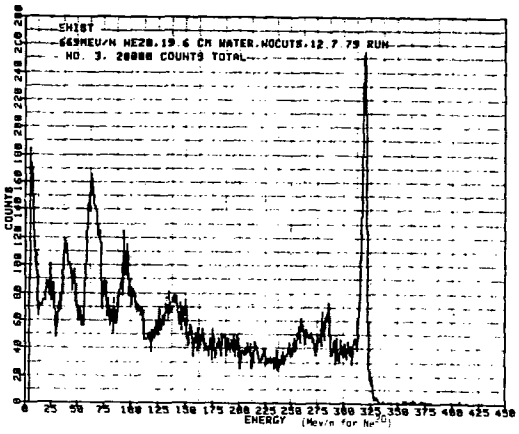

Fig. 5 Residual energy spectrum of a 669 MeV/n ^{20}Ne beam after passing through 19.6 cm of water for a side-entrance detector with amorphous Ge surface coating. The spectrum shows a very large number of counts due to fragments from nuclear reactions during the passage through the water.

The application of an amorphous Germanium coating to the exposed detector surfaces, as developed recently in our Laboratory[2] resulted, however, in a windowless surface with a very good energy collection behavior. Figure 5 shows the energy spectrum of a beam of 669 MeV/n ^{20}Ne after passing through 19.6 cm of water. The observed FWHM is 4 MeV/n. A calculation of the broadening of the monochromatic beam of ^{20}Ne particles due to multiple scattering in 19.6 cm water shows an expected figure of 2.2 MeV/n FWHM. The remaining of the observed peak width may be attributed to statistical fluctuations in the number of light particles generated within the Ge detector by the ^{20}Ne ions, window effects, plasma effects in the detector charge cloud, and beam energy spread.

Figure 6 shows the residual energy collected by the side-entrance detector as a function of the thickness of a water column modulating the energy of the primary beam. The calculated results, which are expected to be good to approximately 3%, are also plotted. The excellent agreement indicates that there are no peculiar effects due to the ions entering the exposed coated surfaces, and that the energy loss of primary heavy ions in Ge is well understood.

The detector has been in use since Nov. 1979 with excellent stability and repeatability. We expect to be able to place two or more side entrance detectors behind each other to achieve the desired total stopping thickness of approximately 30 cm of water equivalent for a human head tomograph, as the first complete instrument.

Imaging Requirements

A number of experiments have been carried out to determine the number of particles needed per unit cross section in order to obtain a tomographic reconstruction of useful quality.

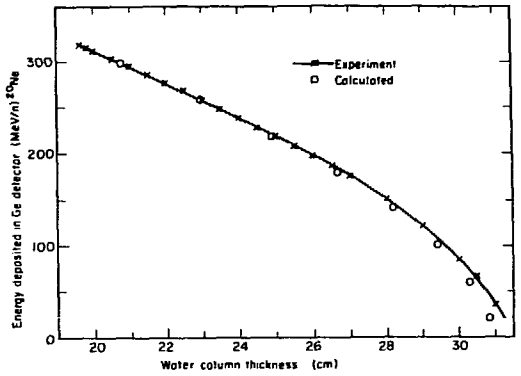

Fig. 6 Energy deposited in a side-entrance Ge detector with surface coating as a function of thickness of a water column modulating the beam energy. The discrepancy at the high thickness end is equivalent to an error of 2% in the energy calibration of the detector electronics.

Data from a 560 MeV/n ^{20}Ne beam experiment were analyzed by defining position bins in the first dE/dx detector and determining the expected error in the determination of the residual energy of the particles in the bins as a function of the number of particles. With a 15 cm water absorber it was found that the standard deviation in six consecutive bins for 200 particles per bin was 0.55 MeV/n, which corresponds to 0.03 cm water. The expected error is then 0.2 percent.

Experiments with 474 MeV/n ^{12}C ions, passing through a 20 cm length of lucite plastic have yielded expected errors in the determination of the water equivalent length of the plastic of 0.07% with 200 particles per bin entering the residual range detector and 0.11% for 100 particles per bin. These figures are very close to the theoretical limit for finding the centroid of a Gaussian shaped peak in the presence of Poisson distributed statistical fluctuations at each point of the peak.[3] They indicate very small systematic errors in the detection process. The residual energy spectra obtained in these measurements contained approximately 30% of the counts in the main primary peak.

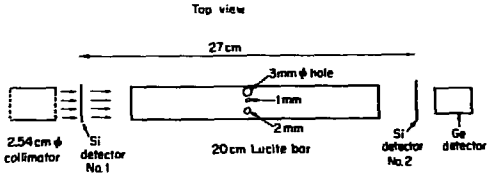

Fig. 7 Experimental setup for study of beam scattering effects and for preliminary examination of one projection.

The use of the second dE/dx detector in the assembly has made it possible to analyze quantitatively the the effect of scattering of primary particles in traversing a certain thickness of material. Figure 7 shows the experimental configuration used in the determination of the beam transport characteristics through a bar of lucite plastic of 20 cm length (23.80 cm water equivalent). In the first experiment, the lucite bar was not placed in its holder, so that the characteristics of the beam delivered by the Bevalac

could be observed. Figure 8a shows a histogram of the offset in transverse position between the two Si detectors for ^{12}C particles of 474 MeV/n, unattenuated except for monitoring chambers and some other moderately thin absorbers in the beam path. The ions would traverse the 3 cm long Ge detector completely. Only ions that would deposit the correct amount of energy in the Ge detector entered in the formation of the graph of Fig. 8a. It shows a near Gaussian distribution with a standard deviation of 0.74 mm. Since detector noise contributes only 0.18 mm position offset uncertainty, the Gaussian width defines the initial quality of the beam. The reasons for this initial observation could be scattering in the several absorbers in the beam path, windows in the dE/dx detectors or characteristics of the beam focusing mechanism of the Bevalac for the particular experimental conditions used.

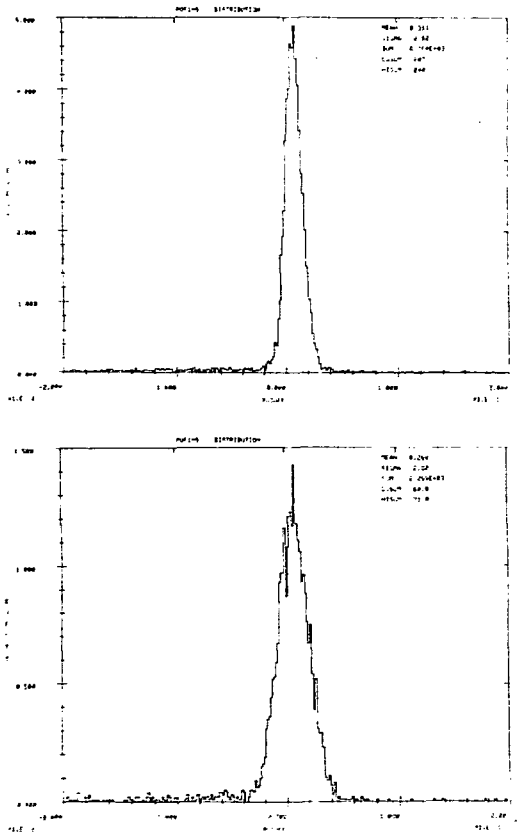

Fig. 8 Position offset histogram between first and second position sensitive dE/dx detectors for a) unattenuated 474 MeV/n ^{12}C ion beam: b) beam passing through a 20 cm bar of lucite.

In a second experiment, the 20 cm bar of lucit was placed in its holder and the above measurements repeated. Only particles that remained ^{12}C upon arrival at the Ge detector entered in the formation of the results. Figure 8b shows the resulting position offset Gaussian, which now has a standard deviation σ = 1.37 mm. The increase in position offset is σ = 1.15 mm due to multiple scattering in the bar, probably magnified by the gap between the bar and the second detector.

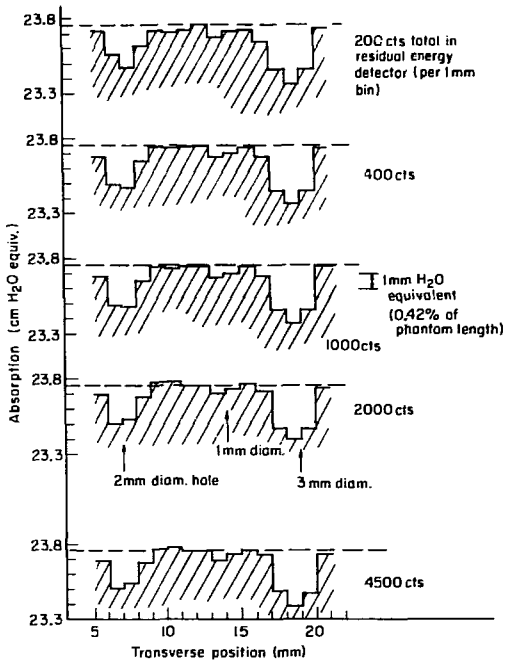

Fig. 9 Results of a single projection experiment in which the three holes shown in Fig. 8 have been imaged with 200, 400, 1000, 2000, and 4500 counts in 1 mm bin.

The effect of the sample scattering on final image quality will be some loss of contrast at high spatial frequencies (or blurring) when the object to be reconstructed is of dimensions comparable to 24 cm of water in absorption. With the same setup of Fig. 7 an initial imaging experiment has been carried out in which three holes of diameters 1, 2, and 3 mm were drilled in a lucite bar of 20 cm length, at approximately midlength, transverse to the beam path as indicated in the figure. The resulting projection has been generated in 16 bins of 1 mm width for approximately 200, 400, 1000, 2000, and 4500 particles per bin. The results are shown in Fig. 9. With the exception of the 1 mm hole with 200 counts per bin, in which statistical uncertainty would make it hard to decide whether the hole can be seen in one single projection, the results show that multiple scattering effects are not felt strongly even with the bin size of 1 mm used in the experiment.

Radiation Dose

The data shown above allows us to estimate average radiation dose to a patient needed to generate an image of a given quality. ^{12}C ions will be used for the estimation, as they give better results and lower dose than ^{20}Ne.

Huesman[4] has shown the statistical error magnification factor in going from one projection to a complete reconstruction for iterative techniques in which a least squares solution has been reached, as a function of number of angles and line integrals per angle. Although iterative techniques may not be the reconstruction technique used ultimately in the present instrument, Huesman's results are found to be quite correct in a more general way if one considers pixel

size to mean the size of a region whose density value is uncorrelated with adjacent regions.[5] For 120 angles, a reconstruction region of 25 cm diameter, an uncorrelated "pixel size" of 0.3 cm and data bins of 0.2 cm width, the error magnification factor is found to be approximately 4.

From the ^{12}C experiments reported above, 100 particles per bin result in an expected error in one projection of 0.11%, or 0.44% in the reconstructed image. This will be considered to be a desirable standard.

For ^{12}C, with an approximate linear energy transfer of 1.5 eV/Å for the plateau region of the depth-dose curve, it is found that

$$\text{Dose} = 2.4 \times 10^{-6} \, N \, n \, / s^2 \quad \text{(rad-gm)}$$

where N is the number of particles needed per bin per view,
n is the number of views required, and
s is the linear size of the data bin in cm.

For the conditions N = 100, n = 120, s = 0.2, the approximate average dose becomes 0.72 Rad-g, substantially below the 1 to 10 Rad-gm which is customarily needed in X-ray CAT scans.

A simple calculation shows that the Ge detector will only need annealing for recovery from radiation damage every 3000 to 6000 complete tomograms. It is expected that annealing will be carried out in the detector cryostat, without disassembly. Radiation damage and annealing of the Si dE/dx detectors is in the process of being studied.

Initial Reconstruction Effort

A first reconstruction experiment has been carried out with a phantom consisting of a 7.3 cm diameter disk of polyethylene with seven 1 mm diameter copper pins arranged along a diameter line, a 2 mm diameter void, and two 5 mm voids filled with 1.05 and 1.10 density solutions of sugar in water. A ^{20}Ne beam of 425 MeV/n passing through a 6 cm water column was used for the experiment. Since the Ge detector has a transverse dimension of only 2.3 cm, the experiment was done by translating the phantom along the transverse axis to six positions separated by 1.5 cm. Using only the center half of the dE/dx detectors, the length of each projection was 9 cm. Rotations were done after the six translation motions of a projection with angular changes of 6°, for a total of 30 angles.

The purpose of the experiment was principally the verification of the complete data taking, analysis and reconstruction procedure, rather than the determination of ultimate accuracy and sensitivity. The copper pins were deemed necessary for verification of position signal amplifier calibrations, and for registration and centering, in spite of the expected artifacts that they would introduce into the image.

Data were acquired until approximately 200 particles were collected per 1 mm bin in the position sensitive detector. From the data given above for a ^{20}Ne beam and an error magnification factor of approximately 12.3 (from Huesman's work), the expected error was calculated to be 2.5%, which should allow visualizing a 1.05 density area if the artifacts due to the presence of the pins would not be overwhelming, which they turned out to be. The average dose was approximately 4 rads., calculated for an average linear energy transfer of 4 ev/Å for ^{20}Ne.

The data were analyzed by forming a 2-dimensional histogram of position in the first dE/dx detector vs residual energy in the Ge detector, with acceptance if the energy deposited in the first detector fell within the Landau peak for primary particles. A 15 x 1024 histogram was thus formed for each one of the six sections of a projection. The 15 energy spectra were then convolved with a ramp filter[3] of sufficient width to accommodate spectra that contained partly "soft" material and partly "hard" material (i.e., the Cu pins). The zero crossing of the convolution determined the estimated residual energy for a 1 mm position bin. The results were then converted to water equivalent thickness by table lookup and stored. The reconstruction algorithm used is a Shepp-Logan filtered back projection with the modifications introduced by Wallingford.[6]

Figure 10a shows the obtained results. There is strong streaking from the pins, the void is quite evident and one can barely detect the 1.1 density region just above the 6th pin from the left. The 1.05 density region, 1 cm above the center line, betwen pins 2 and 3 can perhaps be guessed.

Figure 10b shows a reconstruction carried out from computer generated data without statistical fluctuations or any other imperfections. The effect of the pins is still sufficiently strong that the 1.05 and 1.1 density regions are hard to see.

A comparison of Fig. 10a and 10b shows that the detectors, translation and rotation system, data analysis and reconstruction systems are functioning well and we can now proceed to further experiments to verify the ultimate capabilities of the method.

Conclusion

We have shown that solid state detectors possess the necessary characteristics of accuracy, stability and dynamic range desirable for an instrument for computerized tomography using heavy ions as the probing radiation. Patient dose can be substantially lower than in X-ray CT imaging, particularly with ^{12}C ions. Fundamental to this application for Ge detectors is the absence of surface entrance windows, a condition which we have shown is well attainable.

Further studies will continue before the construction of a clinical instrument can proceed.

Acknowledgements

The authors would like to thank C.A. Tobias, J.C. Fabrikant, F.S. Goulding, and A. Chatterjee for their support and interest in this project.

This paper was prepared under the auspices of the U.S. DOE Contract W-7405-ENG-048 and a grant from the NCI No. CB40302.

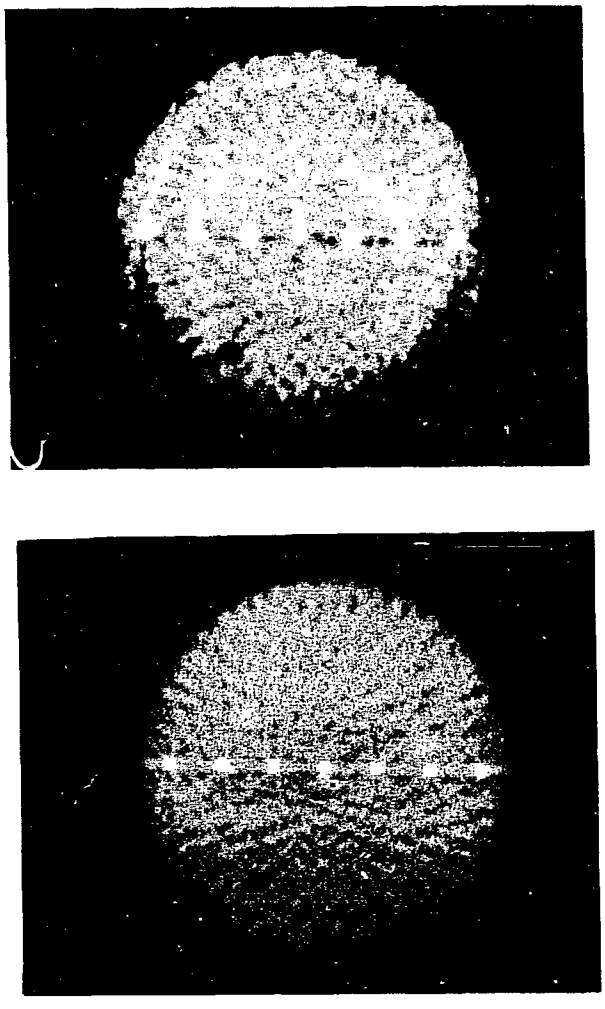

Fig. 10 First reconstruction of a phantom of 7.3 cm diameter (polyethylene) containing seven 1 mm dia copper pins separated by 1 cm to check on centering, registration and spatial linearity of the complete method. A 2 mm void and two regions of 1.05 and 1.1 density are also in the phantom. a) reconstruction from the actual beam experiment; b) reconstruction from perfect computer generated data. Streaking from the pins is predominant in both images, masking the 1.05 and 1.1 density regions almost completely.

References

1. F.G. Sommer, M.P. Copp, C.A. Tobias, E.V. Benton, K.H. Woodruff, R.P. Henke, W. Holly, and H.K. Genant, "Heavy-Ion Radiography: Density and Specimen Radiography", Investigative Radiology, 13, No. 2, pp. 163-170 (1978).

2. W.L. Hansen, E.E. Haller, and G.S. Hubbard, "Protective Surface Coatings on Semiconductor Nuclear Radiation Detectors", IEEE Trans. Nucl. Sci., NS-27, No. 1, pp. 247-251 (1980).

3. J. Llacer, "Optimum Filter for Determination of the Position of an Arbitrary Waveform in the Presence of Noise", NS-28, No. 1 (1981).

4. R.H. Huesman, "The Effects of a Finite Number of Projection Angles and Finite Lateral Samplings of Projections on the Propagation of Statistical Errors in Transverse Section Reconstruction", Phys. Med. Biol., 22, No. 3, pp. 511-521 (1977).

5. R.H. Huesman, Lawrence Berkeley Laboratory, private communication, October 1980.

6. J.S. Wallingford, "An Improved C.A.T. Filter", IEEE Trans. Nucl. Sci., NS-27, No. 1, pp. 954-955 (1980).